A. Benslimane[1], M. Methia[1,2], R. Hammoum[3]

MAGNETO-ELASTIC ANALYSIS OF FUNCTIONALLY GRADED THICK-WALLED SPHERE

[1] Laboratoire Mécanique Matériaux et Energétique (L2ME), Faculté de Technologie, Université de Bejaia, Bejaia 06000, Algérie; e-mail: abdelhakim.benslimane@univ-bejaia.dz
[2] INSA CVL, Univ. Tours, Univ. Orléans, LaMé,3 rue de la chocolaterie, BP 3410, 41034 Blois Cdex, France; e-mail: mounir.methia@univ-bejaia.dz
[3] Institut Clément Ader (ICA), Université de Toulouse, ISAE-SUPAERO, INSA, IMT MINES ALBI, UT III, CNRS, Toulouse, France; e-mail: Roselane.hammoum@isae-supaero.fr

Abstract. An analytical statement of the problem on the magneto-elastic field in the thick-wall sphere made of functionally graded material in the plane strain state is presented. The solid sphere is subjected to internal pressure and a uniform magnetic field. The stress and displacement fields in terms of the radial coordinates considering magneto-elasticity are obtained analytically. Regarding the Maxwell electro-dynamic equations, the Lorentz force function of displacement is expressed in the spherical coordinates. Considering the physical properties of the functionally graded materials as the moduli of elasticity and permeability parameter are varying within a nonlinear general distribution across the thickness while Poisson's ratio is considered constant. The exact solution is obtained by solving the second-order differential equation in terms of displacement derived from the equilibrium equation associated with the Lorentz force. The non-homogeneity parameter is chosen randomly. The obtained results reveal the effect of the magnetic field, gradient parameter, and mechanical loading on the magneto-elastic behavior of the functionally graded spherical thick-wall vessel. Therefore, these parameters have major effects on the radial displacement and radial and circumferential stress components.

Keywords: stress, magneto-elasticity, functionally graded material, thick sphere.

1. Introduction.

The thick-walled spherical vessels are of significant equipment, frequently used in oil, chemical, petroleum, and petrochemical applications and in different industries such as nuclear structures, aerospace and aeronaval structures, civil and mechanical engineering structures, tanks, etc. [1]. Depending on the operation conditions, these vessels can be considered exposed to different solicitations as mechanical, thermal, magnetic or centrifugal forces which have significant effects on displacement, strain, and stress fields and thus on their performance [2]. It is of great importance in solid mechanics to analyze the elastic behavior of such pressurized spherical vessels from the viewpoint of design.

To improve the performance of these spherical vessels within a specific application to their operating conditions, functionally graded materials (FGMs) can be used and replace conventional materials. Indeed, FGMs have become widespread thanks to their controlled spatial distribution of material properties which can help for optimization of the design. The functionally graded materials have attracted interest from scientists and engineers due to their large engineering applications in different fields. FGMs are blend of usually two different materials where a gradually change in the volume fraction of each material changes is observed in some spatial direction [3, 4]. The gradient materials are elastic nonhomogeneous materials with high structural resistance to oxidation and/or corrosion as well as high thermal properties which leads to an increase in their use in different industrial applications [5, 6]. The best choice of the evolution of physical and thermomechanical properties of such materials in one or more spatial directions leads to an optimal properties variation for every specific application [7, 8].

The advantage of the functionally graded materials comparing to the classical composite materials is the absence of interfaces which eliminate the discontinuities of the material properties.

Uniform magnetic field shows its importance and attracted much interest in various scientific and technological fields. It found the application in many biomedical techniques and treatment that require a highly uniform magnetic field [9]. Operation of pressurized vessels under magnetic field leads to a disparate distribution of displacement, strain, and stress fields in comparison with a situation where the mentioned conditions do not exist. Indeed, several studies on the magneto-elastic behaviors of pressurized hollow structures made of FGMs have been reported.

Lutz and Zimmerman [10], Jabbari et al. [6] and additional references can be found where the authors investigate the elastic behavior of pressurized FGM hollow cylinders.

Chen [11] investigated analytically the stress distribution in an isotropic FGM spherical shell under centrifugal forces. Güven and Baykara [12] considered an FGM hollow sphere subjected to internal pressure in the assumption of isotropic linear elasticity. Chen and Lin [13] investigate the elastic field in the case of a thick-walled cylinder/sphere made of exponentially graded materials. Li et al. [14] carried out an elastic analysis for hollow spherical vessels under mechanical loading considering randomly radial nonhomogeneity parameter and using Fredholm integrals to solve the problem. Thick-walled spherical vessels made of linearly and exponentially graded material under mechanical loading was studied by Saidi et al. [15] which developed and exact solution for the displacement and stresses fields. A remarkable work is done by Yıldırım [16], where the author investigated a total of ten material grading rules (linear, power-law, exponential, combined power and exponential…) simultaneously for three types of annular structures (annulus, cylinder and sphere) all of which have the same inner and outer radii under the same mechanical loads.

[17-19] carried out analytical and semi-analytical investigations of thick-walled nonhomogeneous cylinders under different loadings. Cylindrical and spherical vessels made of FGM under pressure and a uniform magnetic field where studied by Dai et al. [17]. They considered physical properties vary in the radial direction across the thickness according to power law distribution. Moreover, they investigated the effects of material nonhomogeneity parameter on the stress distribution and perturbation of magnetic fields. Later, [20] discussed the results obtained by [17]. Loghman and Moradi [21] considered a magnetic field in addition to the electrical charge, temperature and internal pressure on a sphere and investigated stress and displacement fields across the thickness. They showed that the stress distribution can be optimized by selecting an appropriate power index.

Furthermore, some researchers have assumed that the mechanical properties such as the module of elasticity are exponential functions of r. Considering the Poisson's ratio v constant and module of elasticity E an exponential function of r, the authors investigated the stresses and displacements components in FG cylindrical vessels.

In literature, the analytical solutions for elastic field in cylindrical/spherical vessels exist when the magneto-mechanical properties of the material vary as a power law function of the radial position. Moreover, the variation of properties as a power-law function cannot be used in a specific physical problems as the exterior or the interior problems [22] where or $r \to 0$, respectively.

As a continuity of our previous works [23], in this work, an exact solution is presented for the displacement and stress distributions of thick-walled sphere under internal pressure and placed in a uniform magnetic field based in the framework of magneto- elasticity theory. The mathematical formulation of these problems is equivalent, but the physics is different. The material properties are expressed by a nonlinear general form of four parameters and the Poisson's ratio is considered constant. A more general expression was used to take into account the gradient variation of the module of elasticity and magnetic parameter proposed in literature [7]. A second order nonlinear differential equation is derived from the equilibrium equation and has been solved analytically. The magnetoelastic behavior and perturbation of magnetic field vector distributions in the FGM hollow sphere will be calculated.

2. Mathematical problem formulation.

Let us consider sphere made of nonhomogeneous material with, respectively, R_{in} and R_{out} inner and outer radii. Taken into account the geometry of the problem it is more appropriate to consider the spherical coordinate system (r,θ,φ). The sphere is subjected to internal pressure and placed under uniform magnetic field, as Fig. 1 shows.

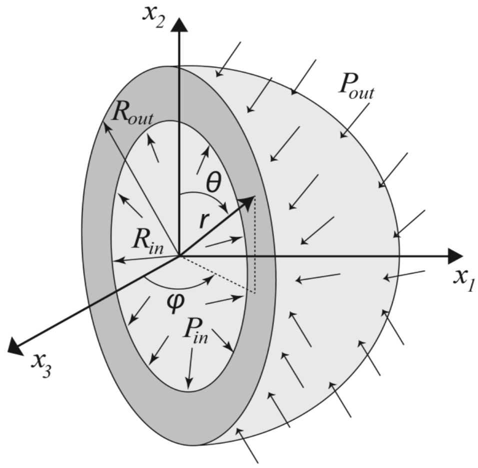

Fig. 1. Three-dimensional nonhomogeneous thick-walled sphere.

The components of displacement can be written in spherical coordinates system as follows:

$$u_r = u_r(r);\ u_\theta = u_\varphi = 0. \tag{1}$$

The strain tensor components may be written in term of the radial displacement component u_i $(i = r, \theta, \varphi)$ such that:

$$\varepsilon_{rr} = \frac{\partial u_r}{\partial r};\ \varepsilon_{\theta\theta} = \varepsilon_{\varphi\varphi} = \frac{u_r}{r};\ \varepsilon_{r\varphi} = \varepsilon_{r\theta} = \varepsilon_{\theta\varphi} = 0. \tag{2}$$

The constitutive relation for linear elastic materials known as Hooke's law is given in the form:

$$\sigma_{ij} = 2\mu(r)\varepsilon_{ij} + \lambda(r)\varepsilon_{ll}\,\delta_{ij}, \tag{3}$$

where $\sigma_{ij} = \sigma_{ij}(r)$ are stress components of Cauchy stress tensor, δ_{ij} is the Kronecker symbol, $\mu(r)$ and $\lambda(r)$ are Lamé's coefficients given by:

$$\mu(r) = \frac{E(r)}{2(1+\nu)};\ \lambda(r) = \frac{\nu E(r)}{(1+\nu)(1-2\nu)}. \tag{4}$$

The material is considered elastic and isotropic. In the assumption of infinitesimally small elastic deformations the Cauchy stress components can be written by substituting the strain tensor component Eq. (2) in the Hook's law given in Eqs. (3) as follows:

$$\begin{gathered}\sigma_{rr} = \left(2\mu(r) + \lambda(r)\right)\varepsilon_{rr} + 2\lambda(r)\varepsilon_{\theta\theta};\\ \sigma_{\theta\theta} = \sigma_{\varphi\varphi} = 2\left(\mu(r) + \lambda(r)\right)\varepsilon_{\theta\theta} + \lambda(r)\varepsilon_{rr},\end{gathered} \tag{5}$$

where $\sigma_{rr}, \sigma_{\theta\theta}$ and $\sigma_{\varphi\varphi}$ are, respectively, the radial and circumferential and meridional component of stress tensor.

The magnetic permeability of the outer surface of the sphere is the same than the magnetic permeability of its surrounding environment. The hollow sphere is assumed non-ferromagnetic and non-ferroelectric and Thompson effect is not taken into account. Therefore, in the presence of an uniform magnetic field $\overrightarrow{H} = (0\ 0\ H_\varphi)$, the electric current density vector $\vec{J}$ and the perturbation of magnetic field vector $\vec{h}$ for a conductive elastic body can be written as follows [10]:

$$\vec{h} = \vec{\nabla} \times (\vec{u} \times \vec{H}); \quad \vec{J} = \vec{\nabla} \times \vec{h}. \tag{6 a, b}$$

In spherical coordinates, Eqs. (6 a) and (6 b) yields to Eqs. (7 a) – (7 d):

$$\vec{u} = (u_r \ 0 \ 0); \quad \vec{h} = (0 \ 0 \ h_\varphi); \quad h_\varphi = -H_\varphi\left(\frac{\partial u_r}{\partial r} + \frac{2u_r}{r}\right); \quad \vec{J} = \left(0 \ -\frac{\partial h_\varphi}{\partial r} \ 0\right). \tag{7 a, b, c, d}$$

Under the effect of the magnetic field, Lorentz magnetic force vector is calculated from the following equation [10]:

$$\vec{f} = \alpha(r)\left(\vec{J} \times \vec{H}\right) = \alpha(r)\left(H_\varphi^2 \frac{\partial}{\partial r}\left(\frac{\partial u_r}{\partial r} + \frac{2u_r}{r}\right) \ 0 \ 0\right). \tag{8}$$

The equilibrium equation for the hollow sphere giving consideration to Lorentz force while the body forces are neglected can be written as follows:

$$\begin{gathered}
\frac{\partial \sigma_{rr}}{\partial r} + \frac{1}{r}\frac{\partial \sigma_{r\theta}}{\partial \theta} + \frac{1}{r\sin\theta}\frac{\partial \sigma_{r\varphi}}{\partial \varphi} + \frac{2\sigma_{rr} - \sigma_{\theta\theta} - \sigma_{\varphi\varphi} + \sigma_{r\theta}\cot\theta}{r} + f_r = 0; \\
\frac{\partial \sigma_{\theta r}}{\partial r} + \frac{1}{r}\frac{\partial \sigma_{\theta\theta}}{\partial \theta} + \frac{1}{r\sin\theta}\frac{\partial \sigma_{\theta\varphi}}{\partial \varphi} + \frac{3\sigma_{r\theta} + \left(\sigma_{\theta\theta} + \sigma_{\varphi\varphi}\right)\cot\theta}{r} + f_\theta = 0; \\
\frac{\partial \sigma_{\varphi r}}{\partial r} + \frac{1}{r}\frac{\partial \sigma_{\varphi\theta}}{\partial \theta} + \frac{\partial \sigma_{\varphi\varphi}}{\partial \varphi} + \frac{3\sigma_{r\varphi} + 2\sigma_{\theta\varphi}\cot\theta}{r} + f_\varphi = 0.
\end{gathered} \tag{9}$$

In the frame work of axisymmetric loadings where all variables are functions of radial position only, the governing equation of the sphere in Eq. 9 yields to a more simplified equation (Eq. 10) in terms of the radial σ_{rr} and circumferential/meridional $(\sigma_{\theta\theta} = \sigma_{\varphi\varphi})$ stresses components is as follows:

$$\frac{\partial \sigma_{rr}}{\partial r} + \frac{2}{r}\left(\sigma_{rr} - \sigma_{\theta\theta}\right) + f_r = 0. \tag{10}$$

By considering the functional expression of module of elasticity and the magnetic permeability the equilibrium equation of the non-homogeneous sphere can be written in terms of the radial displacement. A general expression of gradient material properties is assumed across the thickness of the sphere to take into account the gradient effect of properties [7]:

$$E(r) = E_{in}\left(\frac{r}{R_{in}}\right)^{2m_1} \exp\left(\gamma\left(\frac{r}{R_{in}}\right)^s - 1\right); \quad \alpha(r) = \alpha_{in}\left(\frac{r}{R_{in}}\right)^{2m_2} \exp\left(\gamma\left(\frac{r}{R_{in}}\right)^s - 1\right), \tag{11 a, b}$$

here m_1, m_2, γ and s are constants parameters, E_{in}, α_{in} are the internal coefficients at $r = R_{in}$ of module of elasticity and the magnetic permeability, respectively. The parameters of Eq. (11 a, b) allow wider control in modeling the shape of the material properties compared to other expressions used in literature. With a dataset of $m_1 = m_2 = 0$ or $s = 0,$ respectively, exponential and power-law behaviors can be found. While, for $m_1 = m_2 = 0$ and $s = 0$ taken simultaneously, the expression leads to the homogeneous case.

In order to carry out an investigation of the effect of gradient indexes on the elastic response of the nonhomogeneous hollow sphere placed under a magnetic field, the gradient indexes of the material properties were assumed to be the same, $m_1 = m_2 = m$ where the parameter of inhomogeneity m was assumed to vary from $-2{,}5$ to -1 $(m = -2{,}5; -2; -1{,}5$

and –1). However, the numerical values for *m* was taken arbitrary and do not represent any specific material; four values are considered to reveal the effect of gradient properties on the distribution of the magneto-elastic field and perturbation of magnetic field vector.

For convenience, we consider:

$$2\mu = \xi(\nu)E(r);\ \lambda(r) = \eta(\nu)E(r);\ 2\mu(r)+\lambda(r) = \psi(\nu)E(r), \qquad (12\text{ a, b, c})$$

where:

$$\xi(\nu) = \frac{1}{(1+\nu)};\ \eta(\nu) = \frac{\nu}{(1+\nu)(1-2\nu)};\ \psi(\nu) = \frac{(1-\nu)}{(1+\nu)(1-2\nu)}. \qquad (13\text{ a, b, c})$$

Substituting Eq. (2) into Eq. (3) then into Eq. (10), the second-order differential equation known as Navier's equation can be obtained as follows:

$$\begin{aligned} r^2\frac{d^2u}{dr^2} &+ \left(\frac{\psi\cdot r}{\psi E(r)+H_\varphi^2\alpha(r)}\frac{dE(r)}{dr} + \frac{2(\eta+\xi)\cdot E(r)+2H_\varphi^2\alpha(r)}{\psi E(r)+H_\varphi^2\alpha(r)}\right) r\frac{du}{dr} - \\ &- \left(\frac{2(\eta+\xi)\cdot E(r)+2H_\varphi^2\alpha(r)}{\psi E(r)+H_\varphi^2\alpha(r)} - \frac{\eta\cdot r}{\psi E(r)+H_\varphi^2\alpha(r)}\frac{dE(r)}{dr}\right) u = 0. \end{aligned} \qquad (14)$$

By substituting Eq. (11) in Eq. (14), the differential equation leads to:

$$\begin{aligned} r^2\frac{d^2u}{dr^2} &+ \left(\frac{\left(2(\eta+\xi)+\psi\left(2m+s\gamma\left(\frac{r}{R_{in}}\right)^s\right)\right)\cdot E_{in}+2H_\varphi^2\alpha_{in}}{\psi E_{in}+H_\varphi^2\alpha_{in}}\right) r\frac{du}{dr} - \\ &- \left(\frac{\left(2(\eta+\xi)-\eta\left(2m+s\gamma\left(\frac{r}{R_{in}}\right)^s\right)\right)\cdot E_{in}+2H_\varphi^2\alpha_{in}}{\psi E_{in}+H_\varphi^2\alpha_{in}}\right) u = 0. \end{aligned} \qquad (15)$$

Eq. (15) is the well-known Navier's equation which is in the present case a second order differential equation written in terms of the radial displacement. Therefore, the solution of Eq. (15) can be written as a function of the first $\left(\varphi(a_1, b_1, \xi)\right)$ and second $\left(\phi(a_2, b_2, \xi)\right)$ kind Kummer's functions, respectively, according to [24 – 25]:

$$u(r) = Ar^{\beta_1}e^{-\xi}\varphi(a_1, b_1, \xi) + Br^{\beta_2}e^{-\xi}\phi(a_2, b_2, \xi), \qquad (16)$$

here *A* and *B* are unknown constants which are determined by applying the mechanical boundary conditions.

The first and second kind Kummer's functions can be written, respectively, as follows:

$$\begin{aligned} \varphi(a, b, \xi) &= 1+\frac{a}{b}\frac{\xi}{1!}+\frac{a(1+a)}{b(1+b)}\frac{\xi^2}{2!}+\ldots.+\frac{(a)_n}{(b)_n}\frac{\xi^n}{n!}+\ldots \\ +\phi(a, b, \xi) &= \frac{\pi}{\sin(\pi b)}\left[\frac{\varphi(a, b, \xi)}{\Gamma(1+a-b)\Gamma(b)} - \xi^{1-b}\frac{\varphi(1+a-b, 2-b, \xi)}{\Gamma(2-b)\Gamma(a)}\right]. \end{aligned} \qquad (17)$$

In the above equation, $(a_i)_k = a_i(a_i+1)....(a_i+k-1)$ is Pochhammer's symbol and $\Gamma(\bullet)$ the gamma function.

The arguments of the confluent hypergeometric functions a_i and b_i in equation (15) can be given by:

$$\beta_{1,2} = \frac{\left(\left(\frac{1}{2}-m\right)\psi-\eta-\xi\right)E_{in}-\frac{\alpha_{in}H_\varphi^2}{2}}{\left(\psi E_{in}+\alpha_{in}H_z^2\right)} \pm$$

$$\pm\frac{\sqrt{\left(\left(m-\frac{1}{2}\right)^2\psi^2+\left((1-2m)\eta+(1+2m)\xi\right)\psi+(\eta+\xi)^2\right)E_{in}^2-\left((4m-3)\eta-\left(m+\frac{3}{2}\right)\psi-3\xi\right)\alpha_{in}H_\varphi^2E_{in}+\frac{9}{4}\alpha_{in}^2H_\varphi^4}}{\left(\psi E_{in}+\alpha_{in}H_z^2\right)};$$

(18 a)

$$a_{1,2} = \frac{1}{\psi s\left(\psi E_{in}+\alpha_{in}H_\varphi^2\right)} \pm$$

$$\pm\psi\sqrt{\left(\left(m-\frac{1}{2}\right)^2\psi^2+\left((1-2m)\eta+(1+2m)\xi\right)\psi+(\eta+\xi)^2\right)E_{in}^2-\left((4m-3)\eta-\left(m+\frac{3}{2}\right)\psi-3\xi\right)\alpha_{in}H_\varphi^2E_{in}+\frac{9}{4}\alpha_{in}^2H_\varphi^4+}$$

$$+\left(s+m-\frac{1}{2}\right)\psi^2E_{in}+\left(\left(s+\frac{1}{2}\right)\alpha_{in}H_\varphi^2+(\xi-\eta)E_{in}\right)\psi-2\eta\alpha_{in}H_\varphi^2;$$

(18 b)

$$b_{1,2} = 1\pm$$

$$\pm\frac{2\sqrt{\left(\left(m-\frac{1}{2}\right)^2\psi^2+\left((1-2m)\eta+(1+2m)\xi\right)\psi+(\eta+\xi)^2\right)E_{in}^2-\left((4m-3)\eta-\left(m+\frac{3}{2}\right)\psi-3\xi\right)\alpha_{in}H_\varphi^2E_{in}+\frac{9}{4}\alpha_{in}^2H_\varphi^4}}{s\left(\psi E_{in}+\alpha_{in}H_z^2\right)};$$

(18 c)

$$\xi = \frac{\psi\, E_{in}\gamma\left(\frac{r}{R_{in}}\right)^s}{\psi\, E_{in}+\alpha_{in}H_\varphi^2}. \tag{18 d}$$

The derivative forms of the first and second kind Kummer's functions are given as:

$$\frac{d\phi\left(a_1,b_1,\xi(r)\right)}{dr} =$$

$$= \left(\frac{\frac{d\xi(r)}{dr}}{\xi(r)}\right)\left(\left(\xi(r)+a_1-b_1\right)\phi\left(a_1,b_1,\xi(r)\right)+\left(b_1-a_1\right)\phi\left(-1+a_1,b_1,\xi(r)\right)\right); \tag{19}$$

$$\frac{d\varphi\left(a_2, b_2, \xi(r)\right)}{dr} =$$

$$= \left(\frac{\frac{d\xi(r)}{dr}}{\xi(r)} \right) \left(\left(\xi(r) + a_1 - b_1 \right) \varphi\left(a_2, b_2, \xi(r)\right) - \varphi\left(-1 + a_2, b_2, \xi(r)\right) \right). \tag{20}$$

However:

$$\begin{aligned} \frac{du(r)}{dr} &= \frac{Ar^{\beta_1} e^{-\xi}}{r} \left(\left(\beta_1 - a_1 - b_1 \right) \varphi\left(a_1, b_1, \xi\right) + s\left(b_1 - a_1\right) \varphi\left(-1 + a_1, b_1, \xi\right) \right) + \\ &+ \frac{Br^{\beta_2} e^{-\xi}}{r} \left(\left(\beta_2 - a_2 - b_2 \right) \phi\left(a_2, b_2, \xi\right) - s\,\phi\left(-1 + a_2, b_2, \xi\right) \right). \end{aligned} \tag{21}$$

The radial stress, circumferential stress and perturbation of magnetic field vector components can be calculated by substituting Eq. (16) into Eqs. (5) and (7 b) for hollow sphere made of nonhomogeneous material:

$$\begin{aligned} \sigma_{rr} &= \frac{AE(r)}{r} r^{\beta_1} e^{-\xi} \left(\left(\psi\left(\beta_1 - a_1 - b_1\right) + 2\eta \right) \varphi\left(a_1, b_1, \xi\right) + \psi\, s\left(b_1 - a_1\right) \varphi\left(-1 + a_1, b_1, \xi\right) \right) + \\ &+ \frac{BE(r)}{r} r^{\beta_2} e^{-\xi} \left(\psi\left(\beta_2 - a_2 - b_2\right) + 2\eta \right) \phi\left(a_2, b_2, \xi\right) - \psi\, s\, \phi\left(-1 + a_2, b_2, \xi\right); \end{aligned} \tag{22 a}$$

$$\begin{aligned} \sigma_{\theta\theta} &= \frac{AE(r)}{r} r^{\beta_1} e^{-\xi} \left(\left(\eta\left(\beta_1 - a_1 - b_1\right) + \psi + \eta \right) \varphi\left(a_1, b_1, \xi\right) + \eta s\left(b_1 - a_1\right) \varphi\left(-1 + a_1, b_1, \xi\right) \right) + \\ &+ \frac{BE(r)}{r} r^{\beta_2} e^{-\xi} \left(\eta\left(\beta_2 - a_2 - b_2\right) + \psi + \eta \right) \phi\left(a_2, b_2, \xi\right) - \eta\, s\, \phi\left(-1 + a_2, b_2, \xi\right); \end{aligned} \tag{22 b}$$

$$\begin{aligned} h_\varphi = -H_\varphi \Bigg(&\frac{Ar^{\beta_1} e^{-\xi}}{r} \left(\left(\beta_1 - a_1 - b_1 + 2 \right) \varphi\left(a_1, b_1, \xi\right) + s\left(b_1 - a_1\right) \varphi\left(-1 + a_1, b_1, \xi\right) \right) + \\ &+ \frac{Br^{\beta_2} e^{-\xi}}{r} \left(\left(\beta_2 - a_2 - b_2 + 2 \right) \phi\left(a_2, b_2, \xi\right) - s\phi\left(-1 + a_2, b_2, \xi\right) \right) \Bigg). \end{aligned} \tag{22 c}$$

The constants A and B are determined using the boundary conditions as follows:

$$\sigma_{rr}\big|_{r=R_{in}} = -P_{in}; \; \sigma_{rr}\big|_{r=R_{out}} = -P_{out}. \tag{23}$$

Applying boundary conditions yield a set of linear algebraic equations in terms of *A* and *B*. The unknown coefficients of integration *A* and *B* are calculated by solving the resultant linear algebraic equations.

3. Results and discussions.

3.1. Validation. To confirm the results achieved in this paper, the results were compared with those reported by Ref. [20] in a certain case where the authors assumed a power-law form for the spatial distribution of material properties. They studied the magneto-elastic field of a nonhomogeneous hollow sphere subjected to mechanical loading and placed in a uniform magnetic field.

Let consider a cylinder with $R_{out}/R_{in} = 2$. The numerical values of the gradient material relationship given in Eq. (10) are chosen in the way to reproduce the case examined in [20] i.e. a power-law variation of the module of elasticity and magnetic permeability by considering the constants of the expression as: $\gamma = 0, s = 0$ and $m = -1$.

Fig. 2 illustrates the comparison between the results obtained with the present model and those obtained by Ref. [20]. The figure reveals that a very good agreement is achieved.

3.2. Current Results. Displacement, stresses and perturbation of magnetic field vector are analyzed for the hollow sphere made of FGM under the symmetric mechanical loads. In this section a numerical example is illustrated to analyze the effect of magneto-mechanical field on the elastic response of a sphere obtained by the exact solution derived from the analytical formulation from in the previous section. The effects of the inhomogeneity parameter, the magnetic and mechanical fields on the stress and displacement components are also studied. All the results are obtained using Maple computer program.

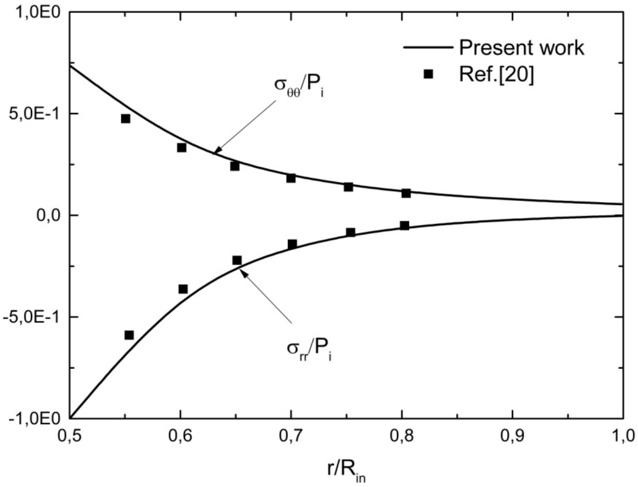

Fig. 2. Comparison between results of present work and Ref. [20] *for dimensionless radial and circumferential stresses in the case of* $R_{out}/R_{in} = 2, \gamma = 0, s = 0$ *and* $m = -1$.

In order to obtain illustrative results, numerical calculations of the material constants for the thick-walled FGM hollow spherical structures are taken as: $R_{out}/R_{in} = 2,$ the module of elasticity at inner radii $E_{in} = 200\,\text{GPa},$ the magnetic permeability coefficient at the inner radii $a_{in} = 1{,}2\;10^{-6}\,\text{H/m},$ the pressure at the inner surface $P_{in} = 500\,\text{MPa},$ the pressure at the outer surface $P_{out} = 0\,\text{MPa}$ and the intensity of the magnetic field $H_{\varphi} = 2{,}23\,10^{9}\,\text{A/m}.$ Poisson's ratio is fixed to $\nu = 0{,}3.$ The material properties of the sphere through the thickness vary only along the *r*-direction.

In order to clarify the analysis and with reference to [7], the constants in Eq. (10) are fixed to: $\gamma = 0{,}172$ and $s = 4{,}1.$ Four values of inhomogeneity parameter are then considered $m = -2{,}5; -2; -1{,}5$ and –1 which correspond to the ratios $E_{in}/E_{out} = 0{,}5, 1, 2$ and 4, respectively. The resulted magneto-elastic field has been normalized and illustrated across the thickness of the sphere to demonstrate the effect of inhomogeneity.

The distribution of the displacement, radial stress, circumferential stress and the perturbation of the magnetic field vector across the thickness of the FGM hollow sphere are illustrated in Figs. 3 – 5, respectively where the results reveal the effect of the inhomogeneity parameter.

Fig. 3 shows the dimensionless radial displacement function of the radial position obtained from the exact solution where different values of inhomogeneity constant m are considered. It can be notice that the maximum and minimum displacements occur at the inner and outer surfaces of the sphere, respectively. Regarding Fig. 3, *a* by raising the inhomogeneity constant *m*, the absolute values of the radial displacement decreases when the intensity of the magnetic field is reduced to zero $(H_\varphi = 0\ \mathrm{A/m})$. This is caused by an increase of the stiffness of the entire thick-walled sphere generated by an increase in the inhomogeneity constant *m*. While, when the intensity of the magnetic field is considered as can be shown in Fig. 3, *b* $(H_\varphi = 2{,}23\,10^9\ \mathrm{A/m})$, the different curves of the dimensionless radial displacement almost coincide. The results shown in Fig. 3, *b* demonstrate the significant effect of the magnetic field on the radial displacement. However, it is obvious to notice that the variation of displacement component in a homogeneous material is similar to that obtained in a heterogeneous material. However, it can be seen that the magnitude of displacement obtained in the case of an FGM spherical structure is higher compared to the displacement magnitude of a sphere made of homogeneous material for the values of m chosen in this work.

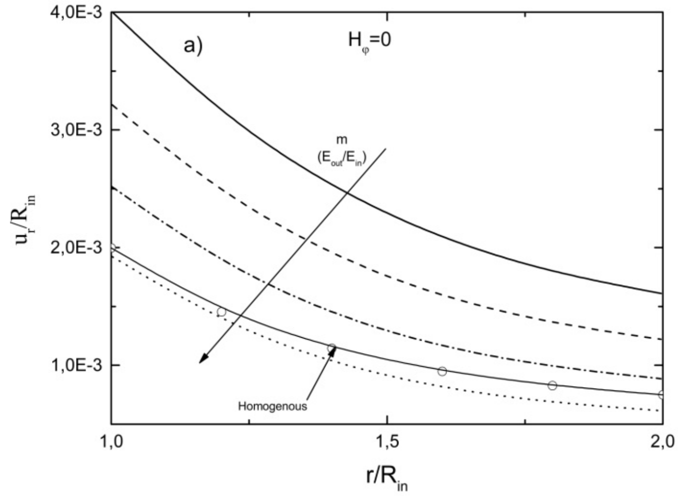

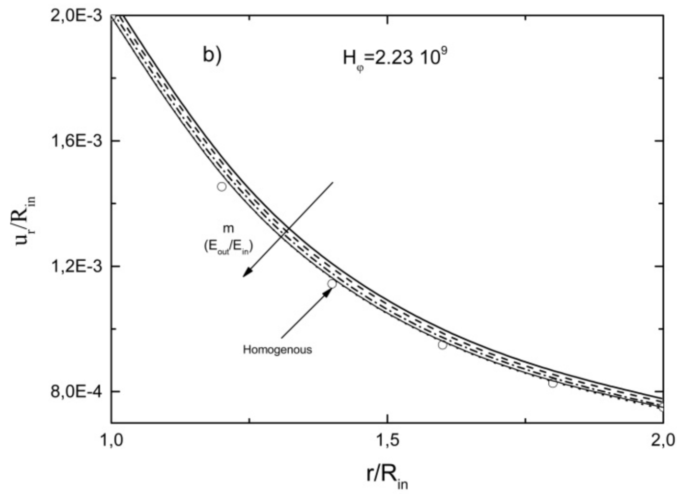

Fig. 3. Radial Distribution of dimensionless radial displacements for different values of inhomogeneity parameter $(m = -2{,}5; -2; -1{,}5$ *and* $-1)$: *a*) $H_\varphi = 0$ *and b*) $H_\varphi = 2{,}23\ 10^9$.

Fig. 4, *a* illustrates the dimensionless radial stress component (Eq. 21 a) with four different values of gradient indexes $(m = -2{,}5; -2; -1{,}5$ and $-1)$. It is obvious to remark from the figure that the homogeneous and heterogeneous materials show similar characteristics concerning the radial stress component. As shown in Fig. 4, *a*, it is obvious to conclude that the radial stress at the internal and external radii of the nonhomogeneous thick-walled sphere satisfy the given asymmetrical boundary conditions of the problem.

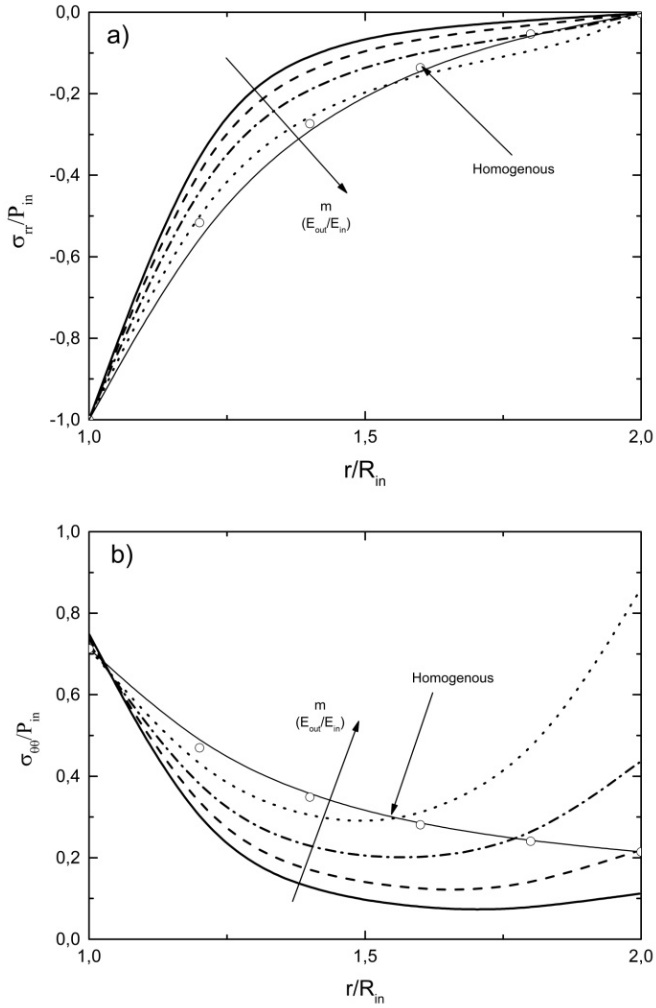

Fig. 4. Distribution of the dimensionless:
a) *radial and b*) *hoop stresses for different values*
of inhomogeneity parameter (m=−2,5; −2; −1,5 *and* −1).

For every nonhomogeneity parameter considered, a monotonic increase of the radial stress can be highlighted in terms of r-direction. Obviously, Fig. 4, *a* reveals that the increase in the absolute values of radial stress is inversely correlated to an increase in the nonhomogeneity constant m which is caused by the increase in the global stiffness of the solid sphere.

Fig. 4, *b* illustrates the distribution of the dimensionless circumferential stress (Eq. 21 a) across the thickness of the sphere. Besides of the value of m, the circumferential stress first decreases and then increases in terms of each value of nonhomogeneity parameter with respect to r (a similar trend is seen in isotropic thick spheres). This is due to the fact that the solid sphere is subjected to only the internal pressure while the external pressure is eliminated. It is also obvious from Fig. 4, *b* that the increase in the absolute values of circumferential stress is proportional to an increase in the nonhomogeneity parameter. As shown in Figs. 4, *a, b*, the magnitude of circumferential stress is larger than that of the radial stress at the same radial position of the FGM hollow sphere.

Fig. 5 illustrates the evolution of perturbation of magnetic field vector. It is clearly seen that the perturbation of magnetic field vector increases gradually from inner to outer radius of the FGM spherical vessel till a certain value than become constant. It can be also seen from Fig. 5 that the absolute values of perturbation of magnetic field vector increase as the nonhomogeneity constant increases.

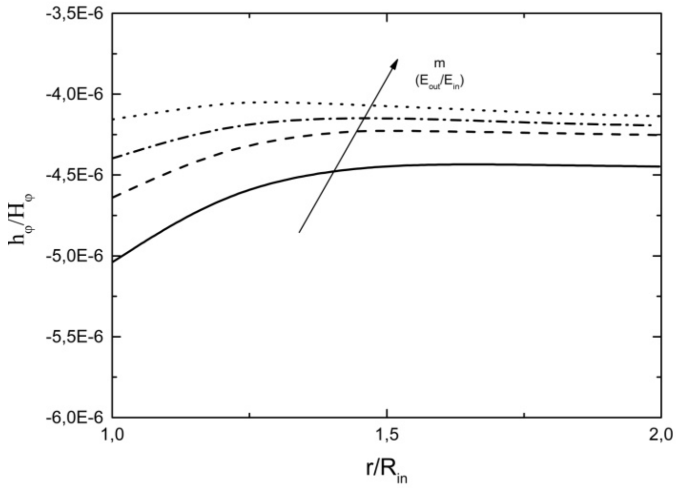

Fig. 5. Radial distribution of h_φ / H_φ for different values of inhomogeneity parameter $m = -2,5; -2; -1,5$ and -1.

Comparing Figs. 4, *a*, *b* and 5 with our previous analysis done on a hollow FGM cylindrical structure [23], it is obviously seen that the evolution of radial stress component through the radial position is nearly the same for an FGM thick-walled spheres and FGM thick-walled cylinders. It is worthwhile to mention from Figs. 4, *b* and 5 that the evolutions of the magnitude of hoop stress and the perturbation of the magnetic field vector components across the thickness have similar characteristics. It is shown that the magnitude of hoop stress in the nonhomogeneous hollow solid sphere is less than the magnitude obtained in the case of the nonhomogeneous hollow solid cylinder, whereas the magnitude of the perturbation of the magnetic field vector in the nonhomogeneous thick-walled spherical structure is higher than the magnitude obtained in the case of nonhomogeneous hollow thick-walled cylindrical structure.

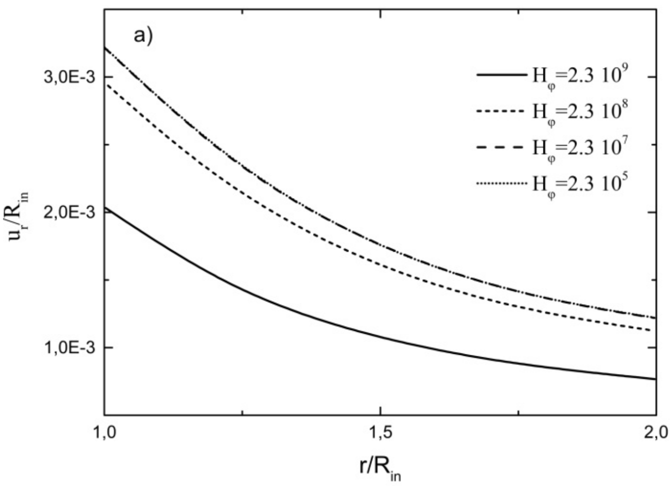

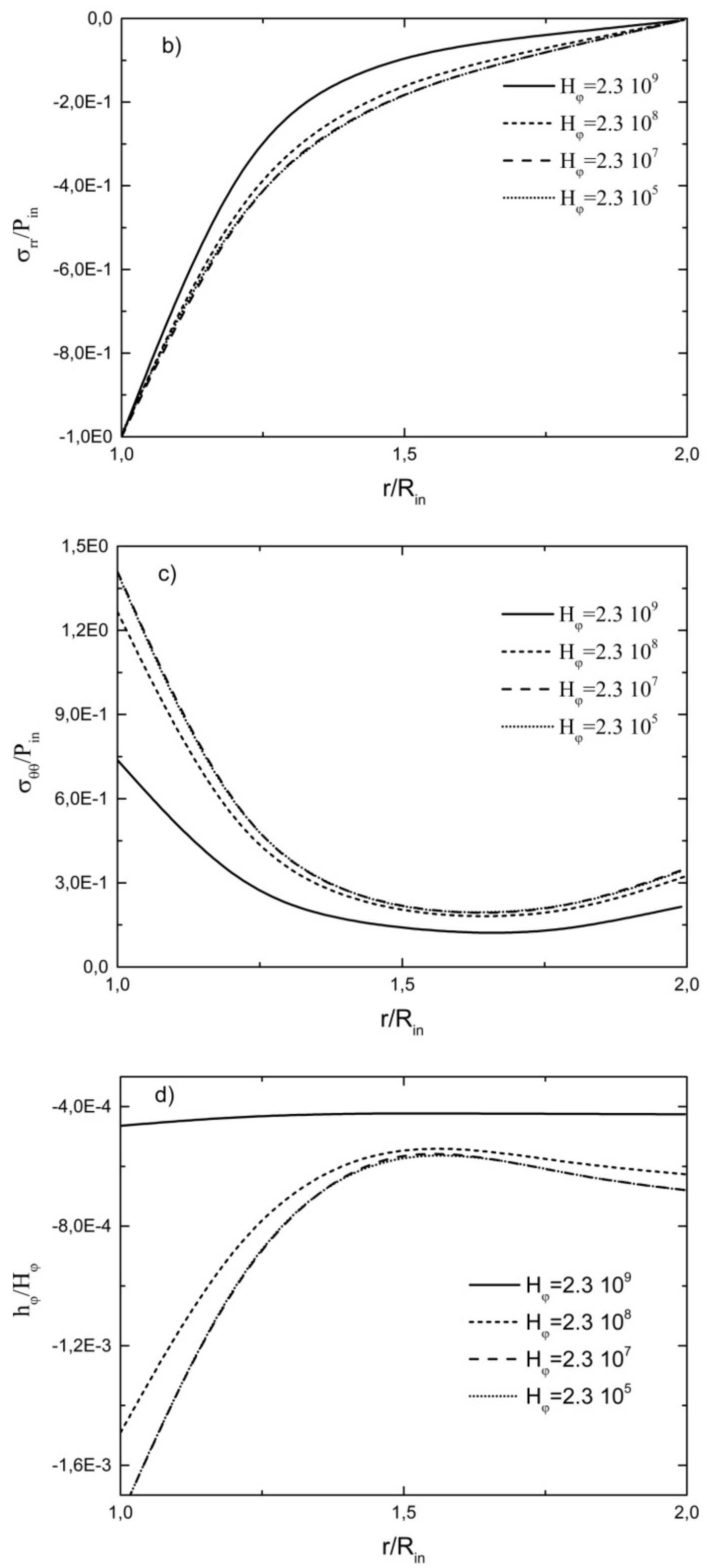

Fig. 6. Magnetic field effects on distributions of displacement, stresses and the perturbation of the magnetic field vector when $m = -2$.

It is shown in Figs. 6, *a, c* that the absolute values of the radial displacement and circumferential stress decrease by increasing the magnetic field intensity while Figs. 6, *b, d* reveal that the absolute values of the magnitude of the radial stress and the perturbation of the magnetic field vector increase as the magnetic field intensity increases. It was further observed that with the values of $H_{\varphi} \le 2{,}3 \cdot 10^{7}$, magnetic field effects are negligible. Moreover, it can be noted that a magnetic field of $H_{\varphi} \le 2{,}3 \cdot 10^{9}$, leaves considerable effects on displacement and stresses distribution.

Conclusions.

In this paper, in the frame work of elasticity theory, exact solutions for FGM hollow spherical structure under a uniform magnetic field and subjected to internal pressure are presented. The effect of the inhomogeneity parameter is analyzed on the distribution of the stresses and displacement fields of the heterogeneous thick-walled spherical structure subjected to internal pressure. A nonlinear general function was used to describe the evolution of the material properties of the FGM sphere across the thickness. The results from homogenous spheres were taken as reference. Displacement and stresses components function of the radial position were illustrated considering different material nonhomogeneity parameters. Numerical results show that the magneto-elastic field and the perturbation of the magnetic field vector are considerably affected by the gradient parameter *m*. Therefore, it can be concluded that with an appropriate choice of the inhomogeneity parameter one can control the stress distribution and design the optimum spherical pressure vessel adjusted to specific applications.

РЕЗЮМЕ. Представлена аналітична постановка задачі про магнітопружне поле в товстостінній сфері, виготовленій з функціонально східчастого матеріалу в стані плоскої деформації. Тверда сфера піддається дії внутрішнього тиску та рівномірного магнітного поля. Поля напружень та переміщення, що враховують магнітопружність, задані в залежності від радіальної координати і отримані аналітично. З врахуванням електродинамічних рівнянь Максвелла функція сили переміщення Лоренца виражається в сферичних координатах. Враховуються такі фізичні властивості функціонально класифікованих матеріалів, як модуль пружності та параметр проникності, які змінюються в межах нелінійного загального розподілу за товщиною, тоді як коефіцієнт Пуассона вважається постійним. Отримано точний розв’язок шляхом розв’язання диференціального рівняння другого порядку щодо переміщення, отриманого з рівняння рівноваги, пов’язаного з силою Лоренца. Параметр неоднорідності вибирається випадковим чином. Отримані результати виявляють вплив магнітного поля, параметра градієнта та механічного навантаження на магнітопружну поведінку функціонально східчастого сферичного товстостінного резервуару. Тому ці параметри мають великий вплив на радіальне зміщення та радіальні і колові компоненти напруження.

КЛЮЧОВІ СЛОВА: напруження, магнітопружність, функціонально східчастий матеріал, товста сфера.

1. *K. Celebi, D. Yarimpabuc, I. Keles.* A novel approach to thermal and mechanical stresses in a FGM cylinder with exponentially varying properties, J. Theor. Appl. Mech. **55**, 343 – 351(2017).
2. *Y. Bayat, H.E. Toussi.* General thermo-elastic solution of radially heterogeneous spherically isotropic rotating sphere, J. of Mech. Sc. and Tech. **29**, (6) 2427 – 2438(2015).
3. *R. Sbulti.* Analytic elastic solutions for pressurized hollow cylinders with internal functionally graded coatings, Composite Structures, **94**, 3592 – 3600, (2012).
4. *M. Ghannad, G.H. Rahimi. M. Zamani Nejad.* Elastic analysis of pressurized thick cylindrical shells with variable thickness made of functionally graded materials, Composites: Part B 45 388 – 396(2013).
5. *F.N. Dehnavi, A. Parzivi.* Investigation of thermo-elasto-plastic behavior of thick walled spherical vessels with inner functionally graded coatings, Meccanica, **52**, 2421–2438(2017).
6. *M. Jabbari, S. Sohrabpour, M.R. Eslami.* Mechanical and thermal stresses in a functionally graded hollow cylinder due to radially symmetric loads, International Journal of Pressure Vessels and Piping, **79**, 493 – 497(2002).

7. *J. Dryden and K. Jayaraman.* Effect of inhomogeneity on the stress in pipes, J. of Elasticity, **8**, 179 – 189(2006).
8. *Z.W. Wang, Q. Zhang, L.Z. Xia, J.T. Wu, P.Q. Liu.* Stress Analysis and parameter optimization of an FGM pressure vessel subjected to thermo-mechanical loadings, Procedia Engineering, **130**, 374 – 389(2015).
9. *M.A. Nemtollah, A. Dini, M. Hosseini.* Thermo-magnetic analysis of thick-walled spherical pressure vessels made of functionally graded materials, Applied Mathematics and Mechanics, **40** (6) 751 – 766 (2019).
10. *R.W. Zimmerman, M.P. Lutz.* Thermal stresses and effective thermal expansion in a uniformly heated functionally graded cylinder, J. of Thermal Stresses, **22**, 177 – 188(1999).
11. *W.Q. Chen.* Stress distribution in a rotating elastic functionally graded material hollow sphere with spherical isotropy, J. Strain Anal., **35**, 13 – 20(2000).
12. *U. Guven, C. Baykara.* On stress distributions in functionally graded isotropic spheres subjected to internal pressure, Mech. Res. Commun., **28**, 277 – 281(2001).
13. *Y.Z. Chen, X.Y. Lin.* Elastic analysis for thick cylinders and spherical pressure vessels made of functionally graded materials, Comput. Mater. Sci., **44**, 581 – 587(2008).
14. *X.F. Li, X.L. Peng, Y.A. Kang.* Pressurized hollow spherical vessels with arbitrary radial nonhomogeneity, AIAA J., **47**, (9): 2262 – 2266(2009).
15. *A.R. Saidi, S.R. Atashipour, E. Jomehzadeh.* Exact elasticity solutions for thick-walled FG spherical pressure vessels with linearly and exponentially varying properties, IJE Trans. A Basics, **22**(4): 405 – 416(2009).
16. *V. Yıldırım.* The best grading pattern selection for the axisymmetric elastic response of pressurized inhomogeneous annular structures (sphere/cylinder/annulus) including rotation, J. of the Brazilian Society of Mechanical Sci. and Engng., 42: 109(2020).
17. *H.L. Dai, Y.M. Fu and Z.M. Dong.* Exact solutions for functionally graded pressure vessels in a uniform magnetic field, Int. J. of Solids and Struct., **43**, 5570 – 5580 (2006).
18. *H.L. Dai, L. Yang and H.Y. Zheng.* Magnetothermoelastic analysis of functionally graded hollow spherical structures under thermal and mechanical loads, Solid State Sci., **13**, 372 – 378 (2011).
19. *M. Hosseini and A. Dini.* Magneto-thermo-elastic response of a rotating functionally graded cylinder. Struct. Engng. and Mechanics, **56**, 137 – 156 (2015).
20. *M.R. Akbari, J. Ghanbari.* Discussion on “Exact solution for functionally graded pressure vessels in uniform magnetic field”, Int. J. of Solids and Struct., 78-79, 216 – 218(2016).
21. *A. Loghman, M. Moradi.* The electro-magneto-thermo-mechanical analysis of a thick walled sphere made of Functionaly Graded Piezoelectric Material, 21st Annual International Conf. on Mechanical Engineering-ISME2013, 7 – 9 May, 2013, Tehran, Iran.
22. *M. Mohammadi, J.R. Dryden.* Influence of the spatial variation of Poisson’s ratio upon the elastic field in nonhomogeneous axisymmetric bodies, Int. J. of Solids and Struct., **46**, 788 – 795 (2009).
23. *A. Benslimane, C. Medjdoub, M. Methia, M. AKhadimallah, D. Hammiche.* Investigation of displacement and stress fields in pressurized thick-walled FGM cylinder under uniform magnetic field, Materials Today: Proceedings, (2020). (DOI: 10.1016/j.matpr.2020.05.462).
24. *M. Abramowitz, A.I. Stegun.* Handbook of Mathematical Functions, Dover Eds, (1970).
25. *W.W. Bell.* Special Functions for Scientists and Engineers, D. Ven Nostand Company Ltd., London, (1968).

From the Editorial Board: The article corresponds completely to submitted manuscript.

Надійшла 26.08.2021 Затверджена до друку 13.12.2022